Title

Energy pile groups for thermal energy storage in unsaturated soils

Authors

Behbehani, Fatemah
McCartney, John S

Publication Date

2022-10-01

DOI

10.1016/j.applthermaleng.2022.119028

Peer reviewed

Applied Thermal Engineering 215 (2022) 119028

Contents lists available at ScienceDirect

Applied Thermal Engineering

journal homepage: www.elsevier.com/locate/apthermeng

Energy pile groups for thermal energy storage in unsaturated soils

Fatemah Behbehani [a], John S. McCartney [b,*]

[a] Department of Civil Engineering College of Engineering and Petroleum Kuwait University Al-Shadadiya, Kuwait
Department of Structural Engineering, University of California San Diego, La Jolla, CA 92093-0085, USA

ARTICLE INFO

Keywords:
Thermal energy storage
Energy pile groups
Unsaturated soils
Enhanced vapor diffusion
Nonisothermal phase change

ABSTRACT

A coupled heat transfer and water flow model implemented in COMSOL and validated against measurements from a tank scale test was applied to investigate the application of energy pile groups for thermal energy storage in unsaturated soil layers. The novel focus of the investigation was understanding the long-term thermo-hydraulic response of the unsaturated soil within the energy pile group during heat injection at high temperature up to 90 °C and associated impacts on the heat storage performance. Unsaturated soil layers are advantageous for thermal energy storage due to enhanced convective heat transfer during injection associated with vapor diffusion and favorable insulation properties during storage associated with lower thermal conductivity of soils surrounding a heat storage system. Evolutions in temperature and degree of saturation in soil layers having different hydraulic properties and water table depths were simulated during five years of operating a group of five energy piles with inlet fluid temperatures of 90 °C during heat injection and 30 °C during heat extraction. Transient fluctuations in the degree of saturation were observed in all soil layers simulated, but a permanent decrease was only observed for a soil layer having a greater air entry suction after several cycles of heating and cooling. While the heat storage in energy pile groups in unsaturated soil layers was always between that of dry and saturated soils with no groundwater flow, the soil hydraulic properties and water table depth were found to control both the rate of heat transfer and the total heat stored. When comparing the performance of energy pile groups with a group of borehole heat exchangers commonly used in heat storage applications, the energy piles were approximately 1.2 times more effective in extracting heat with a faster response confirming their suitability for heat storage.

1. Introduction

Shallow geothermal heat exchangers have been demonstrated to be an efficient, sustainable, and environmentally friendly means of exchanging heat between buildings and the subsurface soil or rock, meaning that they are a promising tool to help reduce carbon emissions associated with building heating and cooling operations. Geothermal heat exchangers are typically installed in widely-spaced boreholes extending to depths on the order of 200 m but in some cases up to 2500 m to seasonally exchange heat with the subsurface without disturbing the mean ground temperature (e.g., [29,66,16,11]). Geothermal heat exchangers can also be used for thermal energy storage applications that have the goal of concentrating heat in the ground in an array of closely spaced boreholes (e.g., [20,55,42,68,6]). While boreholes in rock extending to up to 1000 m have been studied for thermal energy storage (e.g., [68]), most thermal energy storage systems involve boreholes in soil with lengths on the order of 50 m and spacing between 1.5 and 3.0 m.

Issues encountered in using geothermal heat exchangers for thermal energy storage are that they typically must be installed in an array outside a building's footprint, they require a surficial insulation system to minimize upward heat losses, and they must have a sufficiently large number of boreholes to minimize the effects of lateral heat loss into the surrounding subsurface. To address these issues, this study investigates the use of energy piles in unsaturated soils for thermal energy storage. Energy piles are deep foundations that function as both load support and heat exchangers between the ground and an overlying structure [15,13,51,36]. Use of energy piles for thermal energy storage permits efficient use of space beneath a buildings footprint and takes advantage of the facts that energy piles are typically installed beneath a surficial slab or basement that provides insulation from the atmosphere and the surrounding unsaturated soil has lower thermal conductivity than saturated soils minimizing lateral heat losses. Accordingly, this study uses numerical simulations to understand how the thermal energy

* Corresponding author.
E-mail addresses: fatemah.behbehani@ku.edu.kw (F. Behbehani), mccartney@ucsd.edu (J.S. McCartney).

https://doi.org/10.1016/j.applthermaleng.2022.119028
Received 31 December 2021; Received in revised form 24 May 2022; Accepted 15 July 2022
Available online 18 July 2022

storage in energy pile arrays in shallow unsaturated soil profiles can take advantage of enhanced heat injection associated with coupled heat transfer and water flow within the energy pile array and the lower thermal conductivity of the unsaturated soil outside the array [6]. While soil layers have the greatest volumetric heat capacity when saturated with water, groundwater flow commonly occurs in saturated soils which may have an undesired effect on the concentration of heat within an array [18].

Energy piles have a higher heat transfer rate per unit length than borehole heat exchangers due to their larger diameter [14] and may be more cost effective to construct as they take advantage of construction already taking place for building support [15,70,32]. Different from geothermal heat exchangers in boreholes, the length of energy piles is dictated by the structural demand from the building rather than heat exchange requirements, with lengths less than 15 m for low-rise buildings (e.g., [43,44,73,1,36]) but up to 25 m for high-rise buildings (e.g., Laloui et al. 2006, [74,13]). The shorter length of energy piles compared to borehole heat exchangers implies that a greater portion of their length will be within the vadose zone above the water table. While driven, screwed, or cast-in-place deep foundations have been converted to energy piles, most energy piles consist of cast-in-place reinforced concrete with heat exchange tubing in a U shape is placed within the inside perimeter of the reinforcement cage [15]. The larger diameter of energy piles often permits multiple loops to be installed [38]. Although the spacing in energy pile groups is dictated by the structural demands of the building, which may make the group spacing greater than that in borehole heat exchanger arrays, they have larger diameter/length ratios which may permit a greater amount of heat to be concentrated within the energy pile as well as the surrounding soil. Concrete has a specific heat capacity of 960 J/(kgK) that is only slightly higher than that of most soils (800–850 J/kgK), but the density of concrete is greater than that of the backfill grout in borehole heat exchangers, leading to a larger volumetric heat capacity that approaches half that of water. A goal of this study is to compare the thermal energy storage characteristics of arrays of geothermal borehole heat exchangers and energy piles, which may have contrasting responses due to their different geometries even for the same center-center spacing.

While most of the literature on subsurface thermal energy storage systems focused on saturated soil layers due to the greater volumetric heat capacity of saturated soil (e.g., [72,55,23,35]), several studies have found that unsaturated soil layers near the ground surface may be superior for heat storage applications [18,40,5,53]. While some investigations on the behavior of geothermal heat exchangers in unsaturated soils only considered heat transfer by conduction with a thermal conductivity that decreased with the degree of saturation (e.g., [19]), it is well known that the flow of water in liquid and vapor forms may have a significant effect on the surrounding soil thermal response via convection mechanisms [56,5]. Recent studies on thermal energy storage using borehole heat exchangers in unsaturated soils considering the vapor phase change effects focused only on short-term heating and cooling effects on a single borehole heat exchanger [5] and a system of borehole heat exchangers [18,40,6] in their performance evaluation. Başer et al. [5] observed a large decrease in degree of saturation of the soil surrounding a solitary borehole heat exchanger during heating, which was not fully recovered during ambient cooling. However, the magnitude of the decrease in degree of saturation may have been due to the particular temperature boundary conditions and thermo-hydraulic properties of the soil that were investigated in that study. Catolico et al. [18] performed a multi-year analysis of a large borehole heat exchanger array and found that the heat retained within the array increased each year despite heat losses and heat extraction. They found that soil layers with lower thermal conductivity and lower hydraulic conductivity retain heat closer to the heat exchanger and are thus better for heat storage applications. While borehole heat exchangers in unsaturated soil layers have been studied, the thermal performance of energy piles in unsaturated soils has only been investigated through a limited number of laboratory-scale tests [25,2,24] and numerical simulations [9–10,52,53]. Some field-scale energy piles were installed in unsaturated soil layers, but sensors were not incorporated to monitor unsaturated soil effects Murphy et al. 2014, [65]. Although Sani & Singh [53] investigated the long-term cyclic heating and cooling response of energy piles in unsaturated soils, they did not investigate conditions corresponding to thermal energy storage. Energy piles in unsaturated soil layers having different initial soil degrees of saturation and soil properties under the sustained elevated temperatures associated with heat storage requires further study.

While few studies have investigated the use of energy piles for heat storage in saturated soil layers (e.g., [23,35]), they did not investigate the boundary conditions representative of borehole heat exchangers, specifically inlet fluid temperatures greater than 60 °C necessary to effectively concentrate heat in the subsurface (e.g., [55]). Dupray et al. [23] studied heat storage in energy pile arrays but only focused on heat injection rates that led to pile temperatures less than 30 °C. While this is consistent with the maximum temperature encountered in energy piles used for heat exchange applications, it is typical in thermal energy storage systems that a constant inlet fluid temperature of 70 to 90 °C will be encountered when using solar thermal panels as the heat source [18,6]. While a heat exchanger fluid temperature of 90 °C is higher than that typically previously investigated in thermo-mechanical studies on energy piles (Laloui et al. 2006, [13], Murphy et al. 2014), it is expected that the energy piles will have a thermo-elastic response for the types of soils where drilled shaft foundations are typically used (over-consolidated, stiff soil deposits). Extrapolation of the linear trends for different energy piles reported in the literature like those summarized by Murphy et al. (2014) and Olgun and McCartney [41] indicates that thermal deformations and thermal axial stresses during a change in temperature of 60 C will increase by 2–3 times that expected for a change in temperature of 20 °C, but will remain within acceptable limits.

To address the gaps in the literature summarized above, this paper studies the thermal behavior of energy pile groups used for thermal energy storage by evaluating the impact of soil layers having different thermo-hydraulic properties and initial degrees of saturation on the long-term thermal response and heat storage performance of the system. The specific objective of this study is to simulate the transient behavior of unsaturated silt surrounding a group of five energy piles having diameters of 0.9 m and lengths of 15 m separated by 1.5 m. The piles performance was studied over the duration of five heating and cooling seasons and compared to the same soil with different degrees of saturation and water table depths. While saturated soil conditions are used as a basis for comparison, it is assumed that there is no groundwater flow, even though it is known that groundwater flow will have a detrimental effect on heat storage [18] even when it may have a positive impact on heat exchange [34]. Distributions in soil temperature and degree of saturation of the soil at different radial locations within and around the energy pile were assessed over time. The piles performance was evaluated by comparing the heat transfer rate, extracted and stored heat, and changes in energy pile heat extraction in the different soils. To demonstrate the suitability of using energy piles for heat storage applications, a comparison with a similar array of geothermal borehole heat exchangers performance is included when assessing the ground thermal response and the heat storage performance of the different systems.

2. Background

Numerical modeling is an effective and cost-efficient method to study the long-term performance of energy piles considering the complex unsaturated soil coupled heat transfer and fluids flow behavior expected in unsaturated soil layers. In the framework of modeling heat transfer and liquid flow in unsaturated soils, Philip & de Vries [45] were the first to develop a comprehensive model to calculate the thermal and

non-isothermal gradient effects on liquid water and water vapor flow in porous materials and formed the basis for several other studies (e.g., [21,17,59,60,61,62,49]). The impact of the nonequilibrium phase change rate of the water was included later in the model of Smits et al. [56] as a source term in the liquid/vapor water mass balance equations. This phase change rate is used to better capture the transient response of geothermal heat exchangers in unsaturated soils during heating and cooling cycles. The model used by Başer et al. [5] and Başer & McCartney [6] considered thermal effects on the unsaturated soil parameters which made the model dependent on soil temperature and degree of saturation, and then evaluated the behavior of single and multiple borehole heat exchangers in unsaturated soils. Behbehani & McCartney [10] used this model to study a single energy pile in unsaturated soil to understand the permanent effect of heat exchange in unsaturated soil layer with different initial water content. They found that the greatest changes of the degree of saturation in the soil are within 0.2 m from the energy pile interface. Behbehani & McCartney [9] studied the effective stress of energy pile in unsaturated soil layer and found that the thermally induced water flow will leading to an increase in axial pile capacity which will result in a higher restraint against the pile thermal expansion. This implies that coupled heat transfer and water flow should be considered in designing the thermo-mechanical design of energy piles used in heat storage applications with sustained high temperatures up to 90 °C. Faizal et al. [24] performed tank-scale tests on reduced-scale energy piles and found that smaller changes in temperature and degree of saturation occurred during cyclic heating and cooling operations of energy piles compared to monotonic changes in temperature, which emphasize the importance of considering differences in energy pile behavior for heat exchange and heat storage applications. Sani & Singh [53] investigated the long-term behavior of energy pile groups in unsaturated sand and clay layers with constant initial degrees of saturation. They modeled the energy pile groups in 2D and included the water liquid and vapor flow. Their work mostly focused on the changes in soil temperature around the energy piles and the changes in the soil temperature and degree of saturation with depth, but and did not include changes in suction or saturation with depth, or consideration of the pile heat extraction efficiency.

The thermo-mechanical behavior of solitary energy piles has been studied thoroughly using experimental and numerical approaches [13,58,25,75,10]. However, energy piles are typically constructed in groups to support an overlying structure, and energy pile groups may have different thermo-mechanical behavior compared to a solitary energy pile. Although many experiment and numerical studies investigated the thermo-mechanical behavior of energy pile groups (e.g., [50,22,38,47,48,35,46]), their behavior under thermal boundary conditions associated with heat storage has not been well-studied. In unsaturated soils, energy pile groups may have different behavior within the piles group than outside the group due to the combined effects of the piles on the degree of saturation between the piles.

3. Numerical model

The behavior of a group of energy pile or borehole heat exchangers in an unsaturated silt layer was simulated using customized coupled heat transfer and fluid flow modules in unsaturated soils implemented into a COMSOL Multiphysics model. The coupled heat transfer and fluid flow modules were used by Başer et al. [5], Başer & McCartney [6] and Behbehani & McCartney [9] and Moradi et al. [40] to study the behavior of geothermal heat exchangers in unsaturated soils and were originally developed by Smits et al. [56]. The modules include the non-isothermal mas balance equations of liquids in porous media which represent the heat transfer and flow behavior in the porous fluid including the liquid water and the gas, and considers the vapor change rate and mass balance equation. The soil layer is modeled using the solid heat transfer module where the soil heat transfer rate and heat capacity are modeled as functions of degree of saturation. The COMSOL model simulates heat injection into or extraction from the energy piles or borehole heat exchangers via turbulent fluid flow through a closed-loop heat exchanger pipe network embedded within the concrete energy piles or soil-backfilled boreholes, and uses the coupled heat transfer and water flow modules to track the transient changes in soil temperature and degree of saturation which may affect the heat injection, storage, and extraction within the array. This information is used to understand changes in the efficiency of heat extraction of energy pile arrays in unsaturated soils over time.

3.1. Governing equations

The heat transfer balance equation for unsaturated porous media is given as follows [69,40]:

$$\left(\rho C_p\right)\frac{\partial T}{\partial t}+\nabla.\left(\left(\rho_w C_{pw}\right)u_w T+\left(\rho_g C_{pg}\right)u_g T\right)-\nabla.(\lambda\nabla T)=Q-L_w R_{gw} \quad (1)$$

where ρ is the total density of soil, C_p, C_{pw}, and C_{pg} are the volumetric heat capacities of soil, water, and gas, respectively, ρ_w is the density of water as function of temperature [28], ρ_g is the temperature- and pressure-dependent density of gas, λ is the saturation-dependent thermal conductivity of soil, u_w and u_g are the velocity of water and gas, respectively, T is the soil temperature, Q is a heat source, L_w is the latent heat of vaporization [39]), and R_{gw} is the phase change rate between water and vapor due to evaporation or condensation and is calculated as follows [12,71,40]:

$$R_{gw}=\left(\frac{b(S_{rw})RT}{M_w}\right)\left(\rho_{veq}-\rho_v\right) \quad (2)$$

where b is a fitting parameter, R is the universal gas constant, M_w is the water molecular weight, ρ_{veq} is the equilibrium vapor density, ρ_v is the vapor density, and S_{rw} is the degree of water saturation.

The heat transfer balance equation can be simplified for the one fluid case assuming no fluid evaporation or condensation as follows:

$$\left(\rho C_p\right)\frac{\partial T}{\partial t}+\nabla.\left(\left(\rho_w C_{pw}\right)u_w T\right)-\nabla.(\lambda\nabla T)=Q \quad (3)$$

This simplified form can be used to model saturated or dry soil or the concrete pile. The term $\left(\rho C_p\right)\frac{\partial T}{\partial t}$, represents the heat diffusion due to the soil including all the fluids, the term $\nabla.\left(\left(\rho_w C_{pw}\right)u_w T+\left(\rho_g C_{pg}\right)u_g T\right)$ represents the heat convection due to the fluid movement, and it can be neglected in case of dry soil and the concrete pile, and the term $\nabla.(\lambda\nabla T)$ represents conductive heat transfer through the soil including the degree of saturation effects through a degree of saturation-dependent thermal conductivity.

The liquid water nonisothermal mass balance equation in porous media is given as follows [7,27,40,5]:

$$nS_{rw}\frac{\partial\rho_w}{\partial t}+n\rho_w\frac{\partial S_{rw}}{\partial P_c}\frac{\partial P_c}{\partial t}+\nabla.\left[\rho_w\left(-\frac{k_{rw}\kappa}{\mu_w}\right)\left(\nabla P_w+\rho_w g\right)\right]=-R_{gw} \quad (4)$$

where n is the porosity, P_c is the temperature-dependent capillary pressure defined by Grant & Salehzadeh [26], k_{rw} is the relative permeability function for water, κ is the intrinsic permeability, μ_w is the temperature-dependent water dynamic viscosity, P_w is the pore water pressure, g is the acceleration due to gravity, and t is the time. The term in the brackets represents the fluid velocity u_w according to Darcy's Law. The right-hand side and term $n\rho_w\frac{\partial S_{rw}}{\partial P_c}\frac{\partial P_c}{\partial t}$ couples the temperature effects with the fluid flow from Equation (4). The phase change rate in this equation is negative because the increase in temperature will lead to water evaporation.

The nonisothermal gas mass balance equation in porous medium is given by [8,27,40,5]:

$$nS_{rg}\frac{\partial \rho_g}{\partial t}+n\rho_g\frac{\partial S_{rg}}{\partial P_c}\frac{\partial P_c}{\partial t}+\nabla.\left[\rho_g\left(-\frac{k_{rg}\kappa}{\mu_g}\right)\left(\nabla P_g+\rho_g g\right)\right]=R_{gw} \quad (5)$$

where S_{rg} is the degree of gas saturation, ρ_g is the temperature- and pressure-dependent gas density, k_{rg} is the relative permeability function for gas in soil, μ_g is the gas dynamic viscosity, and P_g is the pore gas pressure. This equation has a similar format to the liquid water non-isothermal mass balance equation, but the phase change rate is positive due to water condensation while heating. This equation is ignored when modeling dry or fully saturated soil layers.

The mass balance equation of water vapor is given as follows [56]:

$$n\frac{\partial\left(\rho_g S_{rg} w_v\right)}{\partial t}+\nabla.\left(\rho_g u_g w_v-D_e\rho_g\nabla w_v\right)=R_{gw} \quad (6)$$

where w_v is the mass fraction of water vapor in the gas phase; $D_e=D_v\tau$ is the effective vapor diffusion coefficient, D_v is the diffusion coefficient of water vapor in air, and $\tau=n^{1/3}S_{rg}^{7/3}\eta$ is the tortuosity relationship of Millington & Quirk [37].

The enhancement factor for vapor diffusion η is calculated using the form of the empirical model of Cass et al. [17] used by Smits et al. [56], as follows:

$$\eta=a+3S_{rw}-(a-1)\exp\left\{-\left[\left(1+\frac{2.6}{\sqrt{f_c}}\right)S_{rw}\right]^3\right\} \quad (7)$$

where a is a fitting parameter and f_c is the soil fines content.

Heat transfer from the heat exchanger pipes is modeled using the COMSOL Multiphysics module for nonisothermal pipe flow following the momentum and continuity equations for fluid flow in a pipe defined by Barnard et al. [4] and the energy equation for an incompressible fluid flowing in a pipe defined by Lurie [33].

3.2. Thermo-hydraulic soil properties

The soil investigated in this study is obtained from the Bonny dam on the Colorado–Kansas border. Bonny silt classifies as ML corresponding to the Unified Soil Classification System, has a specific gravity G_s of 2.65, and a maximum dry unit weight γ_d of 16.3 kN/m^3. The SWRC of Bonny silt under elevated temperatures was represented using the model of Grant & Salehzadeh [26] as follows:

$$S_{rw}=S_r+(1-S_r)\left\{\frac{1}{\left[\alpha_{vg}P_c\left(\frac{\beta_0+T_r}{\beta_0+T}\right)\right]^{N_{vg}}+1}\right\}^{(N_{vg}-1)/N_{vg}} \quad (8)$$

where S_r is the residual degree of water saturation, which is assumed to be a function of temperature given by $S_r=S_{r293K}[1-c_{ss}(T-293)]$ where c_{ss} is the She & Sleep [54] fitting parameter, α_{vg} and N_{vg} are van Genuchten [64] fitting parameters, β_0 is the Grant & Salehzadeh [26] fitting parameter equal to −400 K for Bonny silt [3], and T_r is the reference temperature. The SWRC function in Equation (8) can predict the shifts of the residual saturation and the air entry suction due to changes in temperature on the SWRC. The residual degree of water saturation is a key parameter in this model that was found to have a major effect on the coupled heat transfer and water flow process. The hydraulic conductivity function K_{rw} was calculated as follows [64]:

$$K_{rw}=S_{rw}^{1/2}\left[1-\left(1-S_{rw}^{N_{vg}/N_{vg}-1}\right)^{\left(N_{vg}-1\right)/N_{vg}}\right]^2 \quad (9)$$

The soil thermal conductivity variations with the degree of saturation were represented using the model of Lu & Dong [31] as follows:

$$\frac{\lambda-\lambda_d}{\lambda_s-\lambda_d}=1-\left[1+\left(\frac{S_{rw}}{S_f}\right)^m\right]^{1/m-1} \quad (10)$$

where λ_d and λ_s are the thermal conductivity of dry and saturated soil, respectively, S_f is a soil saturation parameter; and m is a pore fluid conductivity parameter. The volumetric heat capacity C_v of unsaturated soil was calculated a similar form to the TCF of Lu & Dong [31] proposed by Başer et al. [5]:

$$\frac{C_v-C_{vd}}{C_{vs}-C_{vd}}=1-\left[1+\left(\frac{S_{rw}}{S_f}\right)^m\right]^{1/m-1} \quad (11)$$

where C_{vd} and C_{vs} are the volumetric heat capacity values of dry and saturated soil, respectively. The key soil thermo-hydraulic properties along with relevant parameters defined at room temperature using the TRIM technique of Wayllace & Lu [67] are shown in Fig. 1.

3.3. Calibration of coupled heat transfer and water flow parameters

A heat injection tank scale test was performed to calibrate the model and to define the fitting parameters. The compacted Bonny silt had a porosity of 0.5, dry density of 13.4 kN/m^3, initial volumetric water content of 18.8 %, and initial temperature of 22.4 °C. While the thermo-hydraulic properties in Fig. 1 could be defined using element-scale tests like that in the TRIM technique, a tank test is necessary to define parameters governing the coupling between heat transfer and water flow. These include the parameters b and a in Equations (2) and (7), respectively, as these two parameters control the speed and the volumetric spreading of the water phase change rate. The tank-scale tests were also useful to define the She & Sleep [54] parameter c_{ss} in the absence of temperature-controlled SWRC measurements.

The soil specimen was prepared by first air drying the soil for 3 days

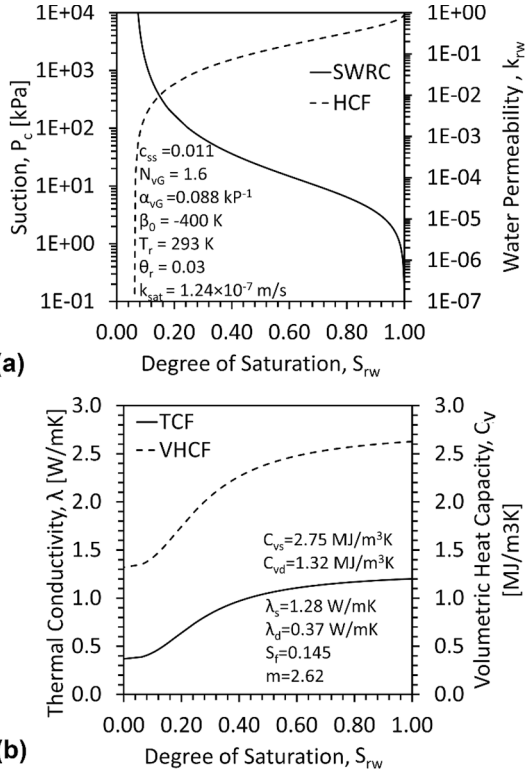

Fig. 1. Bonny silt hydro-thermal constitutive functions: (a) Soil-water retention curve and Hydraulic conductivity function with relevant parameters; (b) Thermal conductivity function and volumetric heat capacity function with relevant parameters.

then screening the soil particles through a No. 8 sieve to remove large particles. The dry soil was then mixed with tap water to reach the target water content of 13 %. Then soil was compacted to a target dry density of 1370 kg/m^3 in four equal weight lefts to a height of 248.7 mm in a cylindrical aluminum container with 555.5 mm diameter and 478.75 mm height as shown in Fig. 2. A cartridge heating element having a diameter of 12.5 mm and a length of 101 mm installed in the center of the soil layer after compacting the first lift was used to heat the soil. Five dielectric sensors (model TEROS 12 from Meter group with 0.1° C resolution and ± (5 % to 8 % dS/m) accuracy) and three thermistors were installed at mid-height in the soil layer at different radial locations shown in Fig. 2 during compaction to track the changes in volumetric water content and temperature, respectively during heat injection. The soil layer was wrapped with plastic wrap to minimize fluid loss and the system was insulated. To perform the tank-scale test, a Watlow controller was used to maintain a temperature of 90 °C at the center of the cartridge heating element until the soil temperature and volumetric water content reached equilibrium, which required approximately 170 h.

As the dielectric sensors are affected by temperature, the volumetric water content data were corrected by first converting the raw volumetric water content values θ_{raw} to dielectric permittivity ε using the Topp [63] equation:

$$\varepsilon = A_T + B_T\theta_{raw} + C_T\theta_{raw}^2 - D_T\theta_{raw}^3 \quad (12)$$

where A_T, B_T, C_T, and D_T are parameters given in Topp [63]. Then, the correction equation of Iezzoni & McCartney [30] was used to calculate the actual dielectric permittivity ε_a as follows:

$$\varepsilon_a = \varepsilon - \Delta T(m_{VWC} + m_d) \quad (13)$$

where m_{VWC} and m_d are temperature correction parameters specific to the dielectric sensor. Finally, the corrected water content θ was calculated as follows:

$$\theta = c_a\varepsilon_a + c_b \quad (14)$$

where c_a and c_b are fitting parameters defined by Iezzoni & McCartney [30] for Bonny silt.

To calibrate the coupled heat transfer and water flow model in COMSOL Multiphysics, the soil was modeled as solid homogenous material with initial saturation of 37.7 %. The initial degree of saturation was calculated by applying constant suction throughout the specimen. The waterproof layer and the tank walls were modeled as no mass flux boundary conditions for liquid and water vapor. The nickel chrome heater boundaries were modeled as heat flux boundary condition that is calculated from the heater's temperature, where the heater thermal conductivity is 8.5 W/m/K. The soil thermal conductivity and heat capacity were modeled using Eq. (10) and Eq. (11). The aluminum tank thermal conductivity and heat capacity are 205 W/m/K and 887 J/kg/K, respectively. The fiberglass Insulation layer thermal conductivity and heat capacity are 0.46 W/m/K and 700 J/kg/K, respectively. The insulation layer was set to the room temperature throughout the full simulation. The simulation was run for the full heating duration of 170 h.

A good match for the temperature and saturation profile and changes with time was found using trial and error by changing a, b, and c_{ss}. Results of the changes in soil temperature and degree of saturation at the location of the middle dielectric sensor of the tank test are shown in Fig. 3. The results of the temperature and degree of saturation with radial distance away from the heating element are shown in Fig. 4. The results and calibrated model match well.

3.4. Model description

In this study, an energy pile group and a group of borehole heat exchangers were simulated over the course of five years involving heating and cooling seasons with equal duration. The model geometries are shown in Fig. 5(a) for the energy pile group and Fig. 5(b) for the borehole heat exchanger group. The group pile model is consisting of five reinforced concrete energy piles with a closed-loop heat exchanger consisting of three vertical U-loops connected in series. The U-loops with each pile have an inlet that are directly connected to the heat pump to generate an equal heating/cooling source per pile. A concrete slab with a width of 5 m, a length of 5 m, and a thickness of 0.9 m was placed above the energy pile group. The slab is assumed to be overlain by a building which provides a thermally insulated upper boundary condition to the energy pile group. The piles are separated by 1.5 m to concentrate heat in the subsurface, with a diameter of 0.9 m, and a length of 15 m are installed in a layer of Bonny silt. The concrete piles have a density of 2400 kg/m^3, a heat capacity of 960 J/(kg·K), and a thermal conductivity of 1.4 W/(m·K). The cross-linked polyethylene (PEX) heat exchanger pipes embedded with the piles and installed about are 0.01 m away from the concrete pile surface. They have a thermal conductivity of 0.48 W/(m·K), a diameter of 44 mm, and a wall thickness of 3 mm. The heat

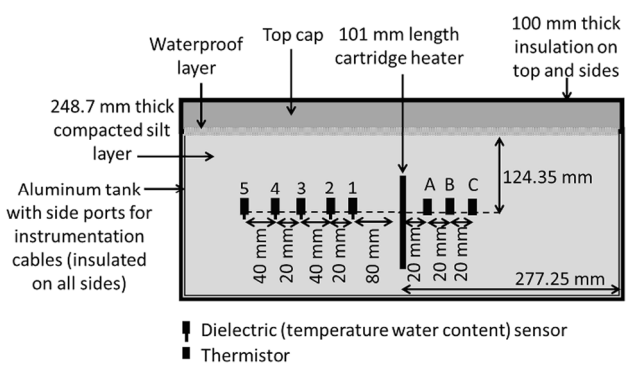

Fig. 2. Cross-sectional view of the tank test and sensor locations used for model calibration.

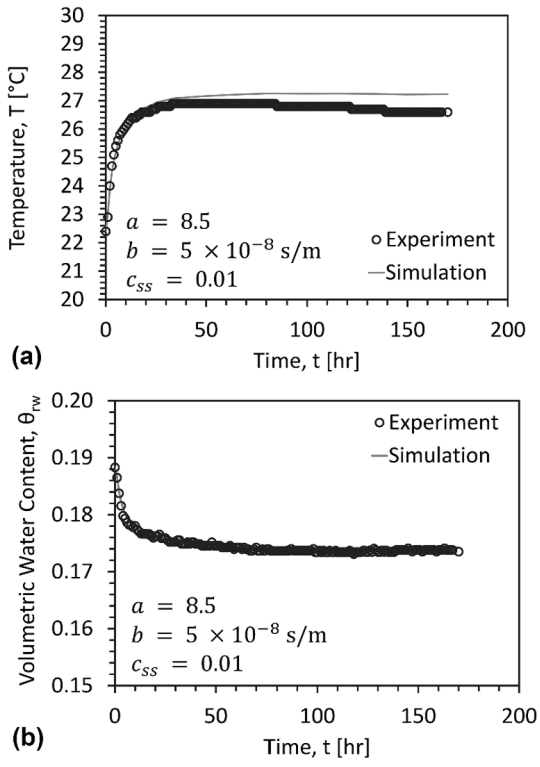

Fig. 3. Predicted and measured time series from the tank-scale heating injection test: (a) Temperature; (b) Degree of saturation.

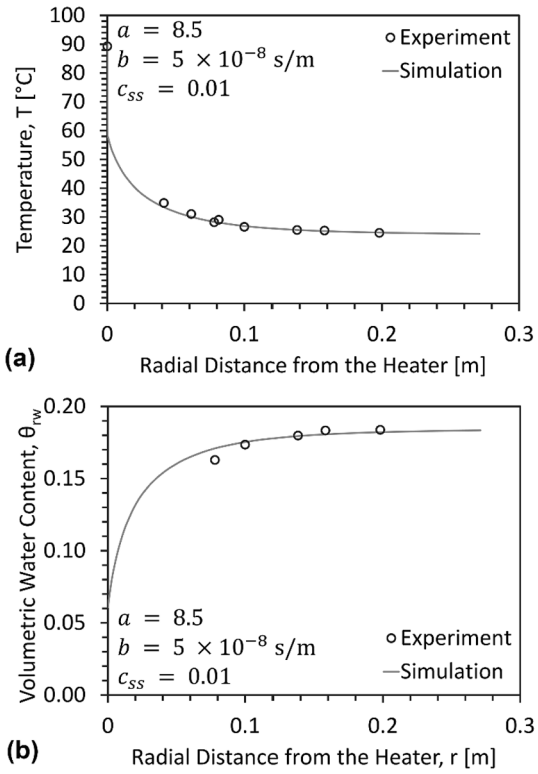

Fig. 4. Horizontal profile of the predicted and measured data at equilibrium from the tank-scale heating injection test: (a) Temperature; (b) Degree of saturation.

exchange fluid is water with a specific heat capacity of 3267 J/(kg·K), and a thermal conductivity of 0.58 W/(m·K). The soil layer is modeled as a cubic box with 20 m length, has initial and boundary temperature of 20 °C, and is thermally insulated with no water and air flux at the boundaries. The soil dimensions and constant temperature boundary condition were found to be suitable to minimize the effects of the outer soil boundaries on the heat transfer and water flow processes near the energy pile group. The soil layer fitting parameters were calibrated from the tank test to be $a = 8.5$, $b = 5 \times 10^{-8}$ s/m, and $c_{ss} = 0.011$. The water table was set at different depths of the soil layer and the SWRC was calculated using residual water content of $\theta_r = 0.03$, $N_{vG} = 1.6$, and four different values of α_{vG} to study the water content and the air entry suction effects on the model. Four cases of unsaturated soil layers were selected with water table depths and parameters as defined in Table 1. Case 0 has a water table at a depth of 10 m (above the tip of the pile) and a value of $\alpha_{vG} = 0.088$ that corresponds to the measured value for Bonny silt. Cases 1, 2, 3 have a water table at the base of the domain of 20 m (below the tip of the pile) and values of $\alpha_{vG} = 0.088, 0.33,$ and 0.88. The initial degree of saturation profiles for the different cases corresponding to hydrostatic conditions are shown in Fig. 6(a).

Table 1
Summary of boundary conditions and key fitting parameters for the unsaturated soil cases evaluated in this study.

Case	Water table depth from surface [m]	van Genuchten [64] fitting parameter α_{vg} [kPa^{-1}]	van Genuchten [64] fitting parameter N_{vg}	She & Sleep [54] parameter c_{ss}	Grant & Salehzadeh [26] β_0 [K]
0	10	0.088	1.6	0.011	−400
1	20	0.088	1.6	0.011	−400
2	20	0.33	1.6	0.011	−400
3	20	0.88	1.6	0.011	−400

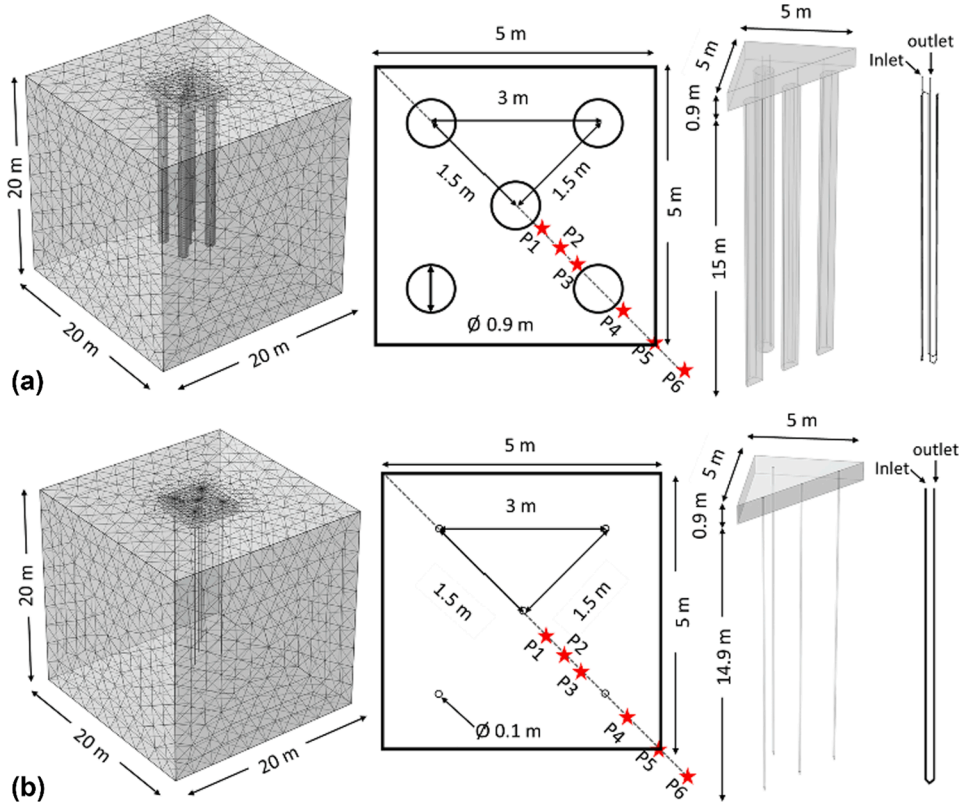

Fig. 5. Model mesh, geometry, and points of interest for analyses: (a) Energy pile group; (b) Borehole heat exchanger group.

The borehole heat exchangers were represented using one loop of PEX heat exchanger pipe with similar properties as the loops in the energy piles. The boreholes have a diameter of 0.1 m and a length of 15 m and are assumed to be backfilled with the same soil as the surrounding deposit (Bonny silt). In a field application sand bentonite would be used as a backfill but using the properties of Bonny silt as the backfill is not expected to have a major effect on the heat transfer from the borehole heat exchangers. The model for the borehole heat exchangers has the same dimensions and initial and boundary conditions as the model for the energy pile group.

A free triangular mesh was generated at the boundaries of the piles and the remaining domain was meshed using free tetrahedral. The mesh has a maximum element size of 2 m and a minimum of 0.02 m. The model mesh for the energy pile group and surrounding soil consists of 201,760 elements and the borehole heat exchanger model mesh consists of 37,886 elements. The mesh was refined near the heat exchanger to accurately capture the soil, water, gas, and the fluid transfer behavior. Simulations were performed for a duration of approximately-five years where the heat exchangers were subjected to a constant heat injection inlet temperature value of 90 °C was applied for six months followed by a constant heat extraction inlet fluid temperature of 30 °C was applied for six months to represent heat storage boundary conditions, as shown in Fig. 6(b). The inlet temperatures were selected to maximize the temperature of the subsurface during heat storage and the reduce the energy cost during heat extraction. The high inlet fluid temperature of 90 °C is consistent with the boundary conditions explored by Welsch et al. [68], and the use of an inlet fluid temperature of 30 °C during heat extraction the need to use a chiller and represents the average temperature of homogenization tanks in the Drake Landing heat storage system [18]. During both heat injection and extraction, the volumetric flow rate for the heat exchange fluid was 100 cm^3/s. This flow rate is sufficient to lead to turbulent flow conditions within the heat exchange tubing (Reynolds number of 3614).

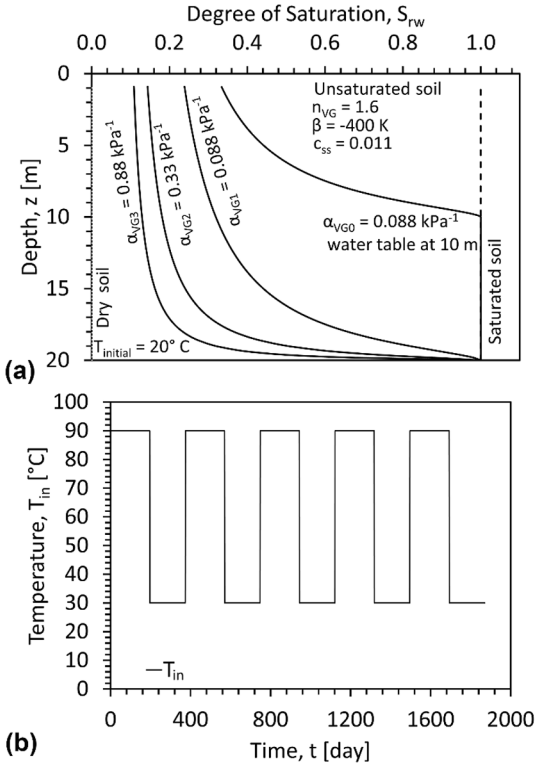

Fig. 6. Key initial and boundary conditions for the simulations: (a) Initial profiles of the degree of saturation along with uniform initial temperature; (b) Inlet fluid temperatures.

4. Results

4.1. Impact of unsaturated soil conditions and thermal load on thermal response

In this study, the results of unsaturated soil surrounding the energy pile group, the pile and the middle borehole thermal performance are investigated. For unsaturated soil properties, the temperature, degree of saturation, thermal conductivity, volumetric heat capacity, mass fraction of water vapor in the gas phase, and evaporation rate are shown for different times and locations. The time series of the changes in soil temperature and degree of saturation for the four saturation cases at different locations are shown in Fig. 7 for the energy pile group and in Fig. 8 for the borehole heat exchanger group. The data points were selected are located 5 m deep, at 0 m from the center pile and the corner pile, at 1.5 m the midpoint between the center and the corner pile, and $15\sqrt{2}$ m away from the center pile as shown in Fig. 5(a) and 5(b). The soil temperature takes a sharp increase in the beginning of the heating cycle; however, it will follow a generally constant path for each heating and cooling cycles, with minimum cumulative changes at P1 and maximum cumulative changes at P6 over the 5 years. The soil will evidently have the maximum changes in temperature at P1 and P3 where the heat is concentrated between the piles and under the slap due to the model geometry. The change in soil temperature is found to very similar for the four cases of the energy pile groups with a maximum average ΔT of 63.5 °C, and the four cases of borehole heat exchanger groups with a maximum average ΔT of 52 °C. Due to lower heat capacity, higher temperature changes were observed in the dryer cases, where Case 4 has the highest change in temperature and Case 0 has the lowest with a maximum different between Case 1 and Case 4 of about 3.2 °C for the energy piles and 2 °C for the borehole heat exchangers. Generally, the soil temperature will have a permanent increase during the thermal loading because the heat exchanger pipe inlet temperature is always higher than the initial soil temperature, which agrees with the observation made by Başer et al. [5]. The changes in the soil saturation are following a reverse pattern to its temperature, however, due to the different air entry suction for the four cases, the change between the cases is evident unlike the temperature profile. For high initial degrees of saturation, the soil will have lower changes in temperature but higher reductions in degree of saturation than the other cases because of the soil air entry suction is high and will reduce the changes in soil saturation with induced suction due to thermal changes. The maximum decrease in the degree of saturation for Case 0 is about 3.4 % more for the energy pile group than the borehole heat exchanger group, and about 1.3 % for Case 4 for the same comparison.

The profiles of temperature and degree of saturation at the end of heat injection and extraction in different years of operation for the energy pile model Case 0 and Case 1 are shown in Fig. 9(a), 9(b), 9(c), and 9(d). The soil temperature profile with depth is dependent on the water-table location, where small uneven change in the temperature can be observed in Fig. 9(a) at 10 m (the water table interface) for Case 0, additionally, faster changes in the soil temperature are observed in Case 0 when comparing storage 1 of Fig. 9 (a) and 9(b). The average permanent increase in unsaturated soil temperature is about 10 °C and 9.5 °C above the water table during the last heat extraction for Case 0 and Case 1, respectively. Along the soil depth, more drying is observed for the high water-table; Case 0. Average permanent reductions in degree of saturation of approximately 3.4 % and 4.4 % are observed in Fig. 9 (c) and 9(d) above the water table during the last heat extraction for Case 0 and Case 1, respectively, this permanent reduction of saturation levels will lead to a decrease in the soil's heat capacity and thermal conductivity and will increase the piles heat transfer efficiency. The radial distribution across the energy pile group cross section shown in Fig. 9(e), 9(f), 9(g), and 9(h). Fig. 9(f) shows a reduction in temperature at 2 to 8 m from the soil boundary during the initial storage for

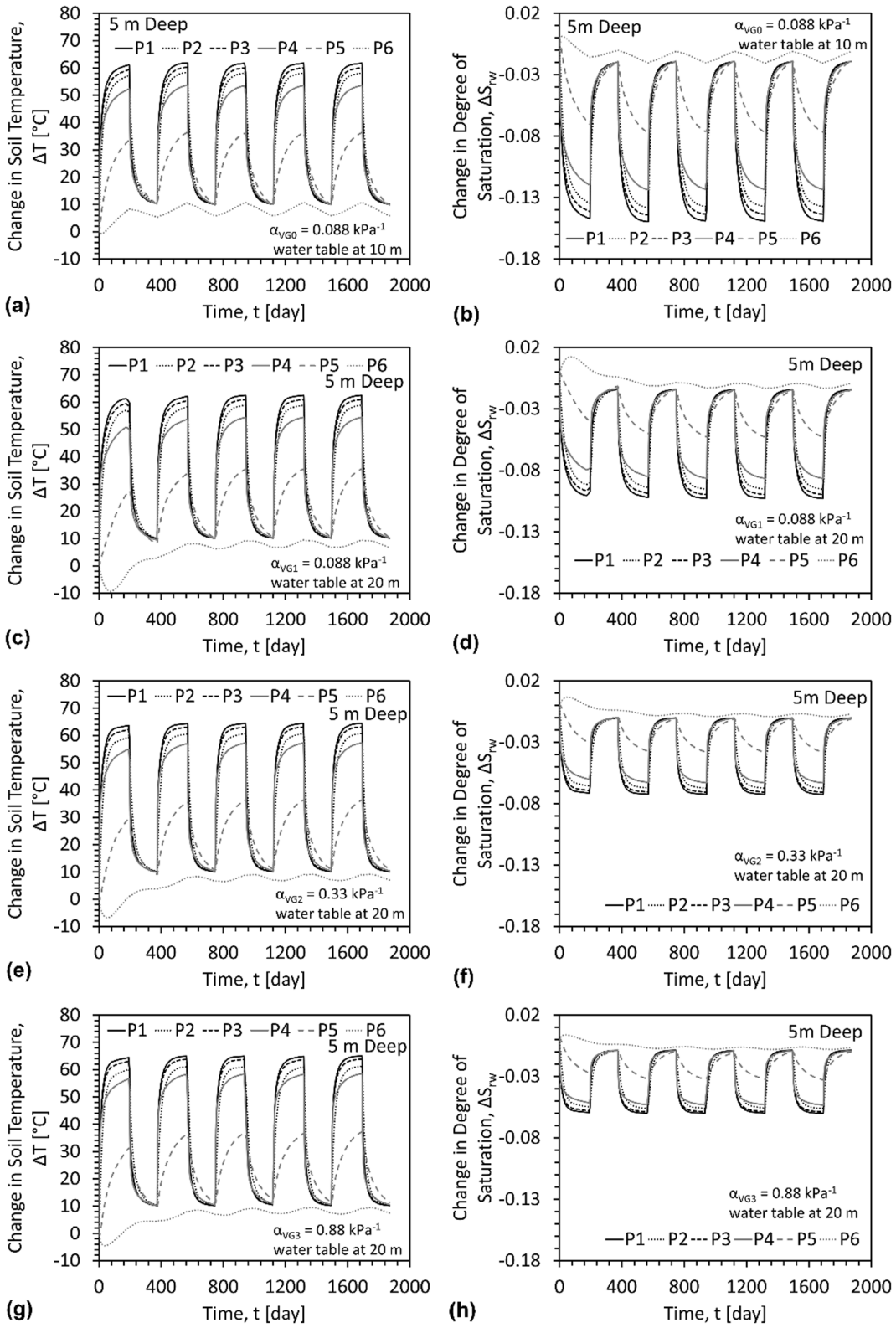

Fig. 7. Energy pile groups model time series results for the changes in: (a) Soil temperature for Case 0, (b) Degree of saturation for Case 0; (c) Soil temperature for Case 1; (d) Degree of saturation for Case 1; (e) Soil temperature for Case 2; (f) Degree of saturation for Case 2; (g) Soil temperature for Case 3; (h) Degree of saturation for Case 3.

Case 1, but this was not observed for Case 0 in Fig. 9(e). This indicates that the temperature is decreasing due to evaporation/condensation rate and the higher suction for Case 1 at a depth of 5 m. Again, the degree of saturation is following a similar pattern for the two cases but with less drying in the low water table case.

The soil's thermal conductivity λ, and heat capacity C_p along the radial distribution across the energy pile group cross section for Case 1 and Case 2 are shown in Fig. 10(a), 10(b), 10(c), and 10(d). The thermal

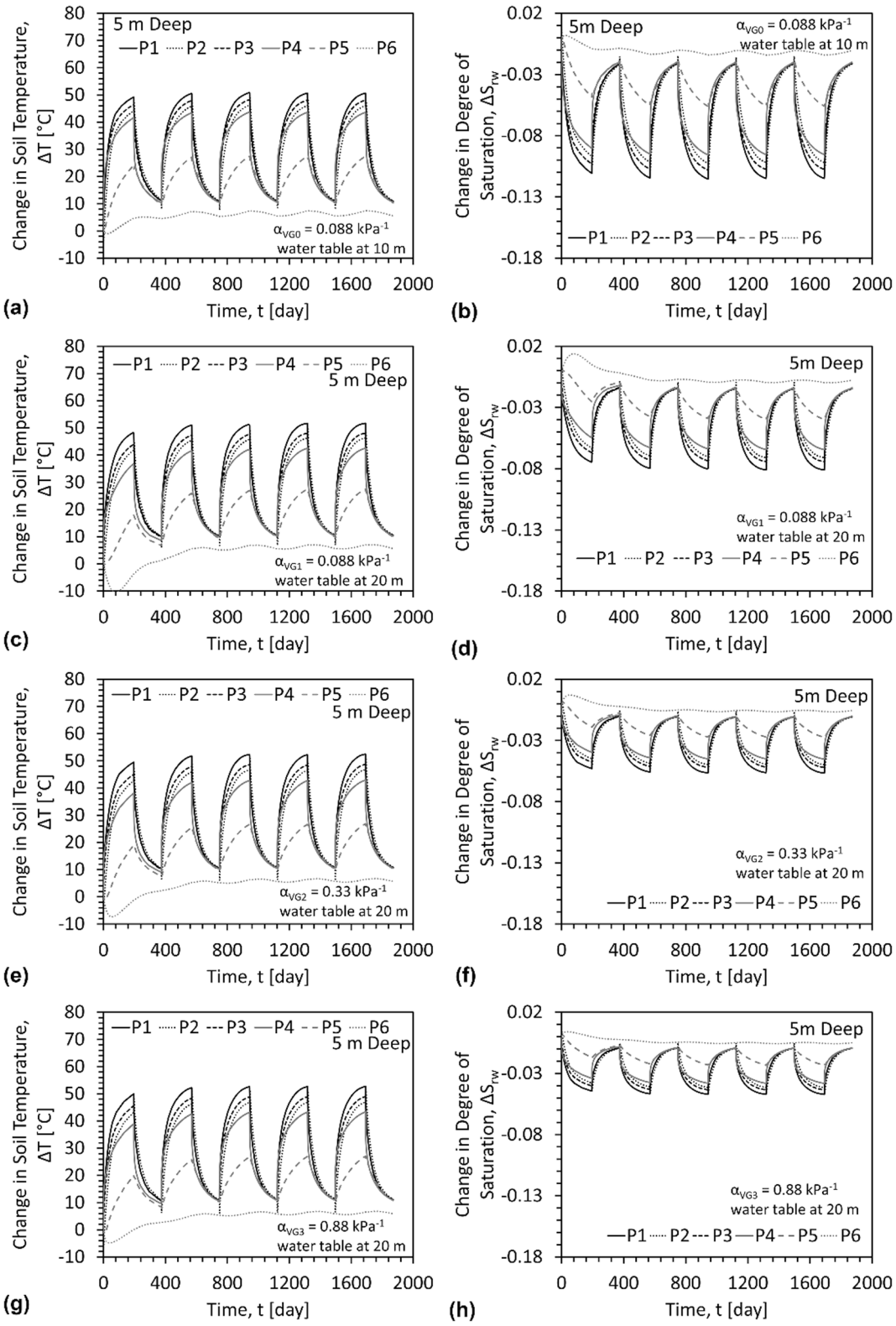

Fig. 8. Borehole heat exchanger group model time series results for the changes in: (a) Soil temperature for Case 0, (b) Degree of saturation for Case 0; (c) Soil temperature for Case 1; (d) Degree of for Case 1; (e) Soil temperature for Case 2; (f) Degree of saturation for Case 2; (g) SOIL temperature for Case 3; (h) Degree of saturation for Case 3.

conductivity and heat capacities of unsaturated soil will follow the same trend as the degree of saturation as shown in the previous Fig. 9(g) and 9 (h) because they are defined as a function of the degree of saturation. Although the degree of saturation changes more along the radial profile for higher water table case than the dryer case as shown in Fig. 9(g) and 9(h), the thermal conductivity and the volumetric heat capacity shown in Fig. 10 exhibit less changes for the for Case 0 than Case 1, because more water will gradually change the thermal behavior. Fig. 11(a) and

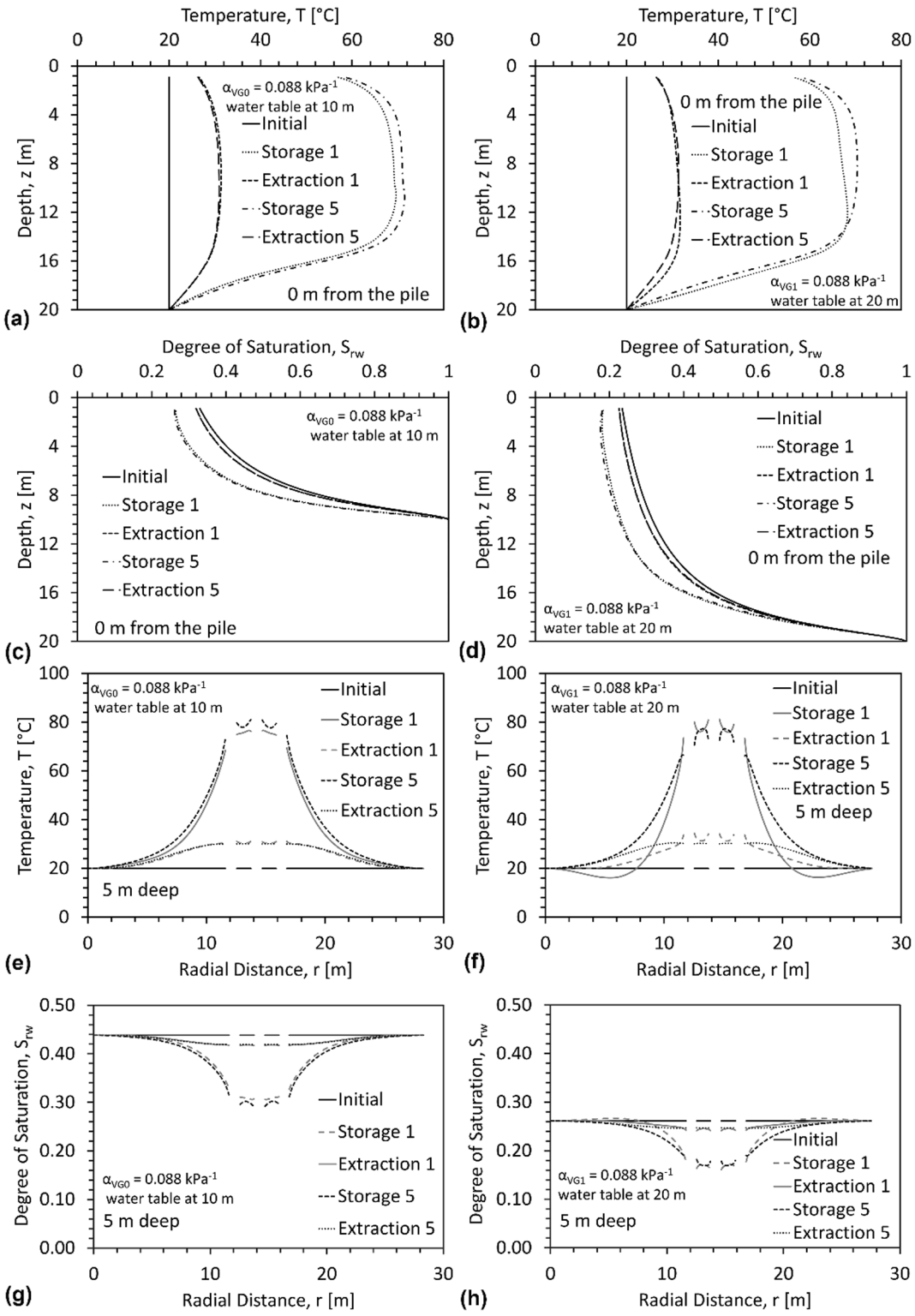

Fig. 9. Results at the end of heat injection and heat extraction for (a) Temperature profile for Case 0; (b) Temperature profile for Case 1; (c) Degree of saturation profile for Case 0; (d) Degree of saturation profile for Case 1; (e) Radial temperature for Case 0; (f) Radial temperature for Case 1; (g) Radial degree of saturation for Case 0; (h) Radial degree of saturation for Case 1.

11(b) show the evaporation/condensation rate at the end of the first and last extreme seasons. The water always evaporates for this model as the ambient temperature is warmer than the ground temperature during heat extraction. This explains the added water vapor in Fig. 11(c) and 11 (d), which increases with the degree of saturation and the evaporation rate and concentrated near the energy piles. The small increase in the water vapor mass in the gas phase is equivalent to the decrease of the degree of saturation as there is no boundary water mass flux.

4.2. *Impact of unsaturated conditions on the efficiency of heat storage*

The thermal performance of the geothermal structures was evaluated

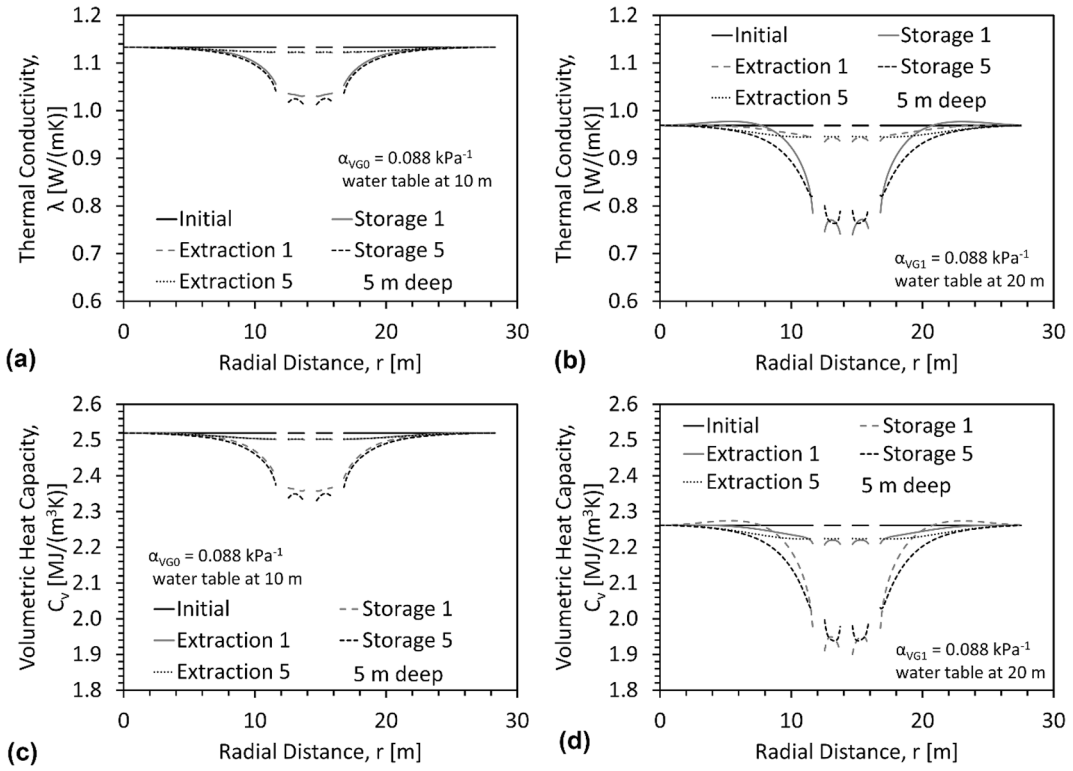

Fig. 10. Radial results at the end of heat injection and heat extraction for: (a) Thermal conductivity for Case 0; (b) Thermal conductivity for Case 1; (c) Volumetric heat capacity for Case 0; (d) Volumetric heat capacity for Case 1.

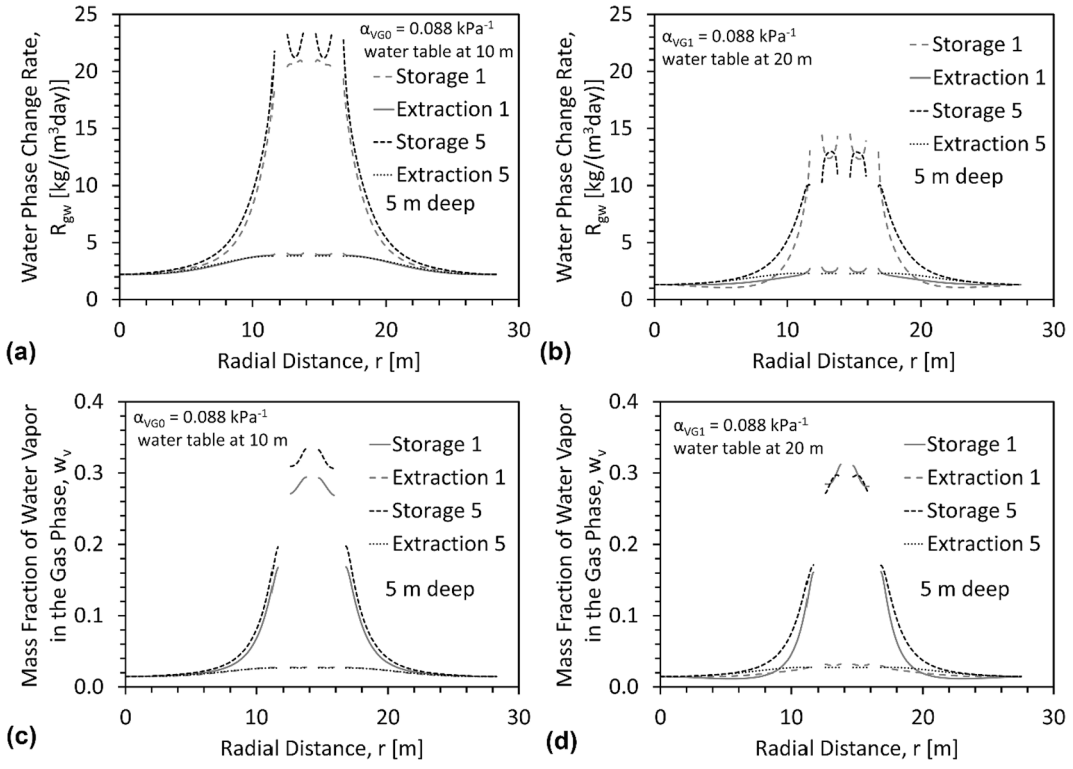

Fig. 11. Radial results at the end of heat injection and heat extraction for: (a) Water phase change rate for Case 0; (b) Water phase change rate for Case 1; (c) Water vapor mass fraction in the gas phase for Case 0; (d) Water vapor mass fraction in the gas phase for Case 1.

by calculating the heat transfer rate and the storage efficiency of the middle pile and borehole. The heat transfer rate is given as follows:

$$\dot{Q} = \dot{V}_w \rho_w C_w (T_{in} - T_{out}) \quad (15)$$

where $\dot{V}_w$ is the volumetric flow rate of the heat exchanger fluid, and T_{in} and T_{out} are the inlet and outlet fluid temperatures. The heat transfer rates for the energy pile group and the borehole heat exchanger group for the four unsaturated soil cases are shown in Fig. 12, along with the cases for dry and saturated soil. Although, heat transfer rate is increases with soil capacity, unsaturated soils heat transfer rate is also affected by the vapor transfer. Heat transfer rate reaches its lowest value in dry conditions due to low specific heat capacity for both energy piles and boreholes. However, the heat transfer rate in unsaturated soils may approach that of saturated soils in case of high air entry suction due to high water vapor transfer. This is an important observation as groundwater flow will likely occur in saturated soil layers, negatively affecting the heat storage, while groundwater flow is not expected in unsaturated soils. The average heat transfer rate of the piles reaches a minimum for the dry soil where it is about 0.45, 0.46, 0.62, and 0.66 times the heat transfer in the unsaturated soil in Case 0, Case 1, Case 2, and Case 3, respectively and about 1.77 the saturated soil. The heat transfer rate in the piles overall is approximately 1.2 times higher than for the borehole heat exchangers, with the maximum difference for the dryer soils and minimum for nearly saturated soils. It is important to note that the water phase change rate and latent heat of vaporization influences the heat transfer rate in the unsaturated soil beside the soil capacity, which may result in higher heat transfer rate for unsaturated soils at low suctions than saturated soils. The transient heat transfer in unsaturated soil is dependent on the degree of saturation, and when the saturation levels increase there will be more fluid flow and more heat loss to the surrounding, however, in dry cases the soil will have higher temperatures near the pile and less influenced range.

The heat transfer rate curves in Fig. 12 were integrated with time to define the total annual amounts of extracted and the injected heat,

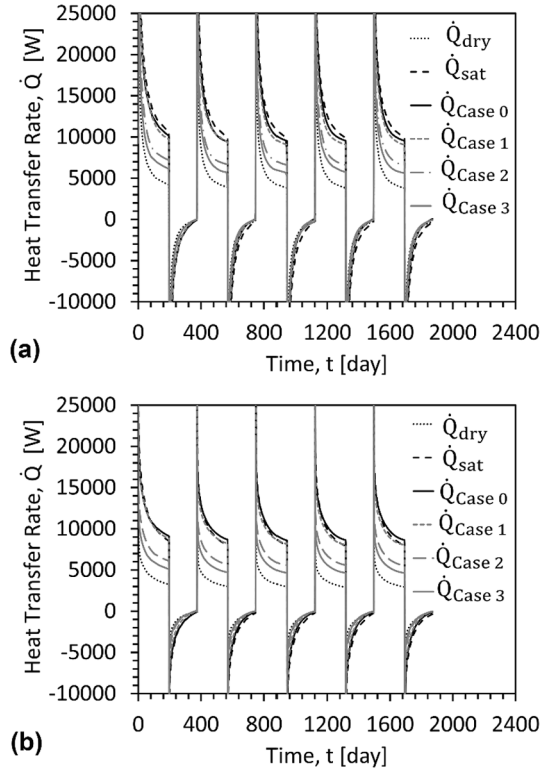

Fig. 12. Heat transfer rates: (a) Energy pile group; (b) Borehole heat exchanger group.

which are shown in Fig. 13(a), 13(b), 13(c), and 13(d). In all the evaluated scenarios, the temperature of the soil layer increased over the course of several annual heat injection/extraction cycles in all soil layers investigated. This means that the soil layers store more heat than in subsequent years because the heat storage depends on the difference between the elevated ground temperature and the ambient ground temperature prior to heat injection. The stored heat is lowest for the dryer soil due to its low heat capacity, despite the lower thermal conductivity. The extracted heat for both scenarios evaluated is better in the unsaturated soil layer in Case 0, and it increases with each year while the stored heat is reduced with year due to the permanent reduction in soil volumetric heat capacity as shown in Fig. 10(c) and 10(d). It is clear from the results that energy piles are storing and extracting more thermal energy than borehole heat exchangers with the same spacing. This can be attributed to the geometry of the energy piles, the thermal properties of the concrete, and the fact that the energy piles have multiple U-loop heat exchangers while the boreholes have only one U-loop heat exchanger.

Another way to study the heat storage in the subsurface is to evaluate the amount of heat stored in the subsurface at the end of the heat injection and heat extraction phases. This may be a better approach to understanding the thermal response of a thermal energy storage system because it captures the overall response of the soil around the heat exchange system. Claesson and Hellström [20] calculated the average thermal storage capacity of soil by defining a cylindrical storage region with the diameter covering the soil having steady state temperature, as follows:

$$Q_s = (T_b - T_a) C_v \pi r^2 H \quad (16)$$

where $(T_b - T_a)$ is the average temperature difference between storage and surrounding subsurface, r is the radius of a cylindrical storage volume, H is the height of the storage volume within the subsurface. The storage capacity was calculated for a cylinder including all the thermal energy storage units with a radius of 3 m and 15 m height. The average temperature difference was calculated per day for the same storage volume using COMSOL Multiphysics, and the stored temperature were taken at the end of each heating and cooling cycles to find the stored capacities. The stored heat per year for the investigated soil layers are shown in Fig. 13(e) and 13(f) at the end of heat injections and 13(g) and 13(h) at the end of heat extractions. For the same storage volume, the energy pile group stored about 1.3 more heat in the duration of five years during heat injection than the borehole heat exchanger group, however, soil will return 1.3 times more heat to the group energy pile during extraction than to the borehole heat exchanger group, leading to more energy stored in the ground surrounding the boreholes during heat extraction. The soil layers with low heat capacity stored the minimum thermal energy while the saturated soil layer stored the most. The saturated soil will have about the double the dry soil storage capacity in the given domain, and the unsaturated soil will have about 1.6, 1.4, 1.2, and 1.1 capacity times the dry soil during heat injection for Case 0, Case 1, Case 2, and Case3, respectively. Case 0 has a different storage behavior during heat extraction in the first year as shown in Fig. 13(g) and 13(h). The higher initial storage capacity could be due to the water table level with the saturated part of the soil layer storing more heat initially. Fig. 13 can sum the heat loss in this system to two parts; heat loss to the heat exchanger pipes and the ground during injection as in Fig. 13(a) and 13(b); and to the ground during extraction as in Fig. 13(g) and 13(h), however, the total heat loss due to spreading is not calculated here as it is not included in the storage volume.

Although it is possible to calculate an efficiency of the heat storage systems by dividing the heat extracted by the heat injected as done by Catolico et al. [18], this calculation may be misleading because the total amounts of heat injected is partially stored and partially lost to the ground meaning that the injected heat is defined as a part of the total injected heat and it will not represent the total input energy to the

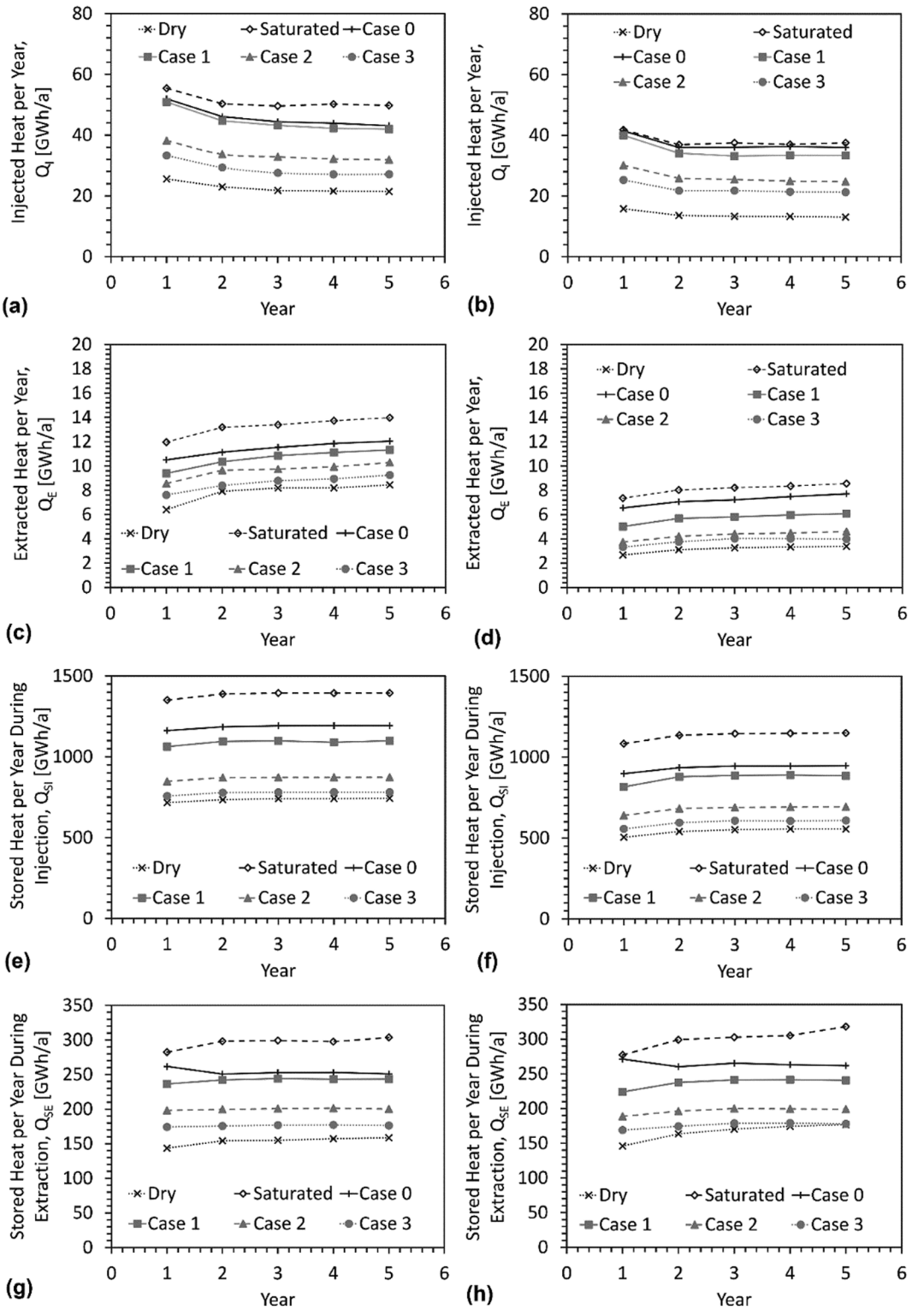

Fig. 13. Thermal performance per year: (a) Heat injected for energy piles; (b) Heat injected for boreholes; (c) Heat extracted for energy piles; (d) Heat extracted for boreholes; (e) Stored heat during injection for energy piles; (f) Stored heat during injection for boreholes; (g) Stored heat during extraction for energy piles; (h) Stored heat during extraction for boreholes.

system. Instead, the efficiency was calculated as follows:

$$\eta_{he} = \frac{|Q_E|}{Q_T} \tag{17}$$

where Q_T is the total thermal energy input into the system calculated using the inlet fluid temperature time history in Fig. 6(b). The annual efficiency trends shown in Fig. 14 follows a similar pattern to the extracted heat for the two systems, where the saturated soils have highest efficiency and the dry soils have the lowest efficiency. The efficiency for the heat storage systems in unsaturated soil layers depends on the depth of the water table and the hydraulic properties of the soil layer. Although dry soils have the lowest heat loss due to the low

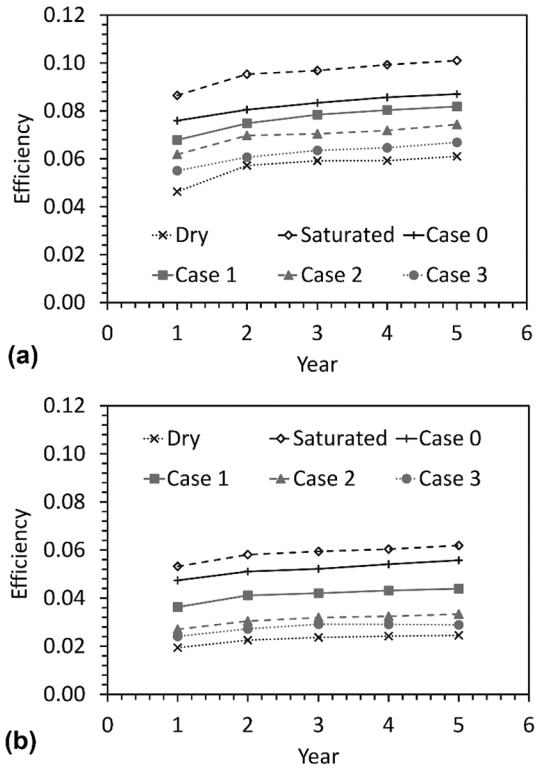

Fig. 14. Evolution in efficiency: (a) Energy pile group; (b) Borehole heat exchanger group.

thermal conductivity, heat storage systems in saturated soil layers tend to have higher operational efficiency and more extracted heat as more heat is stored in the ground near the heat exchangers. Similarly, the efficiency of the embedded piles in unsaturated soil layers will reduce as the soil gets dryer until it reaches the lowest extracted temperature for dry soils. Also, the borehole heat exchanger array will have lower efficiency than energy piles due to the lower surrounding temperatures. Overall, these results emphasize the importance of properly understanding the subsurface hydrological setting on the long-term performance of thermal energy storage systems using either energy piles or borehole heat exchangers.

5. Conclusion

This study focused on the simulation of long-term coupled heat transfer and water flow in an unsaturated silt layer surrounding a group of five energy piles. The effects of different saturation conditions in the silt layer as well as variations in key hydraulic properties of the silt were investigated to understand the impact of unsaturated conditions on the heat transfer rate and water flow in the unsaturated soil layer and the thermal performance of the energy pile group when used as a heat storage system. A three-dimensional numerical model was developed using COMSOL Multiphysics to simulate the non-isothermal heat transfer, water flow, and the vapor diffusion in the unsaturated soil and the model parameters were calibrated by good fitting the of the temperature and saturation profile to a tank scale test. The calibrated model provided novel insights into the conditions in unsaturated soil layers affecting the transient heat injection and extraction processes in both energy pile and borehole groups. Similar changes in temperature for different saturation conditions were found for the unsaturated soil cases with maximum changes in initially dryer locations in the soil layer. Large transient changes in degree of saturation were observed during heat injection. The magnitude of the change in degree of saturation depends on both the heat injection temperature as well as the initial degree of saturation of the soil, and only in some cases does a permanent change in degree of saturation occur during cyclic heating and cooling. The degree of saturation will generally follow a similar pattern to the soil temperature, but initial conditions and the evaporation rate will control the changes in water content as well. The dryer the soil becomes, the higher the changes in temperature, the thermal conductivity, and the heat capacity, however, the lower the changes in water content. Heat transfer in unsaturated soils, even with low degrees of saturation, is less than that in dry soil because of enhanced vapor diffusion. The amount of heat extraction is greater for dry soil due to its lower thermal conductivity and less heat transfer away from the pile group. The thermal performance of the group piles decreases with the increase of the air entry suction and the rise of the water table. Dry soil will store less temperature than unsaturated or saturated soils in a storage range due to its low heat capacity, while the saturated soils will store the most, as long as there is no groundwater flow. Although the results show that energy piles can be used for heat storage, changes in pile capacity, restraint, and thermal stresses during application of these high temperatures associated with heat storage should be studied further in field studies.

The authors declare that they have no known competing financial interests or personal relationships that could have appeared to influence the work reported in this paper.

CRediT authorship contribution statement

Fatemah Behbehani: Conceptualization, Methodology, Investigation, Formal analysis, Visualization, Writing – original draft. **John S. McCartney:** Supervision, Resources, Funding acquisition, Project administration, Conceptualization, Methodology, Writing – review & editing.

Declaration of Competing Interest

The authors declare that they have no known competing financial interests or personal relationships that could have appeared to influence the work reported in this paper.

Acknowledgements

The first author acknowledges the scholarship and support provided by Kuwait University.

References

[1] S.L. Abdelaziz, T.Y. Ozudogru, Selection of the design temperature change for energy piles, Appl. Therm. Eng. 107 (2016) 1036–1045.
[2] G.A. Akrouch, M. Sánchez, J.L. Briaud, Effect of the unsaturated soil condition on the thermal efficiency of energy piles, in: *IFCEE 2015*, ASCE, Reston, VA, 2015, pp. 1618-1627.
[3] N.A. Alsherif, J.S. McCartney, Thermal behaviour of unsaturated silt at high suction magnitudes, Géotechnique 65 (9) (2015) 703–716.
[4] A.C.L. Barnard, W.A. Hunt, W.P. Timlake, E. Varley, A theory of fluid flow in compliant tubes, Biophys. J. 6 (6) (1966) 717–724.
[5] T. Başer, Y. Dong, A.M. Moradi, N. Lu, K. Smits, S. Ge, D. Tartakovsky, J. S. McCartney, Role of nonequilibrium water vapor diffusion in thermal energy storage systems in the vadose zone, J. Geotech. Geoenviron. Eng. 144 (7) (2018), https://doi.org/10.1061/(ASCE)GT.1943-5606.0001910.
[6] T. Başer, J.S. McCartney, Transient evaluation of a soil-borehole thermal energy storage system, Renewable Energy 147 (2020) 2582–2598.
[7] J. Bear, Dynamics of Fluids in Porous Media, Dover, Mineola, NY, 1972.
[8] J. Bear, J. Bensabat, A. Nir, Heat and mass transfer in unsaturated porous-media at a hot boundary. One-dimensional analytical model, Transp. Porous Media 6 (1991) 281–298.
[9] F. Behbehani, J.S. McCartney, Impacts of unsaturated conditions on the ultimate capacity of energy piles, *EUnsat 2020: The 4th European Conference on Unsaturated Soils*. Lisbon, Portugal. Jun. 24-26. pp. E3S Web of Conferences. Les Ulis, France, 195, 04005, 2020a.
[10] F. Behbehani, J.S. McCartney, Simulation of the thermo-hydraulic response of energy piles in unsaturated soils, *Proc. 2nd International Conference on Energy Geotechnics*. E3S Web of Conferences, Les Ulis, France. 205, 05002, 2020b.

[11] R.A. Beier, Thermal response tests on deep borehole heat exchangers with geothermal gradient, Appl. Therm. Eng. 178 (2020) 115447, https://doi.org/10.1016/j.applthermaleng.2020.115447.
[12] N.E. Bixler, NORIA: A Finite Element Computer Program for Analyzing Water, Vapor, Air and Energy Transport in Porous Media, Sandia National Laboratories, Albuquerque, NM, 1985.
[13] P.J. Bourne-Webb, B. Amatya, K. Soga, T. Amis, C. Davidson, P. Payne, Energy pile test at Lambeth College, London: geotechnical and thermodynamic aspects of pile response to heat cycles, Géotechnique 59 (3) (2009) 237–248.
[14] D. Bozis, K. Papakostas, N. Kyriakis, On the evaluation of design parameters effects on the heat transfer efficiency of energy piles, Energy Build. 43 (4) (2011) 1020–1029.
[15] H. Brandl, Energy foundations and other thermo-active ground structures, Géotechnique 56 (2) (2006) 81–122.
[16] W. Cai, F. Wang, J. Liu, Z. Wang, Z. Ma, Experimental and numerical investigation of heat transfer performance and sustainability of deep borehole heat exchangers coupled with ground source heat pump systems, Appl. Therm. Eng. 149 (2019) 975–986.
[17] A. Cass, G.S. Campbell, T.L. Jones, Enhancement of thermal water vapor diffusion in soil, SSSA J. 48 (1) (1984) 25–32.
[18] N. Catolico, S. Ge, J.S. McCartney, Numerical modeling of a soil-borehole thermal energy storage system, Vadose Zone J. 15 (1) (2016) 1–17.
[19] J.C. Choi, S.R. Lee, D.S. Lee, Numerical simulation of vertical ground heat exchangers: intermittent operation in unsaturated soil conditions, Comput. Geotech. 38 (8) (2011) 949–958.
[20] J. Claesson, G. Hellstrom, Model studies of duct storage systems, in: J.P. Millhone, E.H. Willis (Eds.), New energy conservation technologies and their commercialization, Springer, Berlin, 1981, pp. 762–778.
[21] D.A. de Vries, Simultaneous transfer of heat and moisture in porous media, Eos, Trans. Am. Geophys. Union 39 (5) (1958) 909–916.
[22] A. Di Donna, L. Laloui, Numerical analysis of the geotechnical behaviour of energy piles, Int. J. Numer. Anal. Meth. Geomech. 39 (8) (2015) 861–888.
[23] F. Dupray, L. Laloui, A. Kazangba, Numerical analysis of seasonal heat storage in an energy pile foundation, Comput. Geotech. 55 (2014) 67–77.
[24] M. Faizal, A. Bouazza, J.S. McCartney, Thermo-hydraulic responses of unsaturated sand around a model energy pile, J. Geotech. Geoenviron. Eng. 147 (10) (2021) 04021105.
[25] J.C. Goode III, J.S. McCartney, Centrifuge modeling of end-restraint effects in energy foundations, J. Geotech. Geoenviron. Eng. 141 (8) (2015) 04015034.
[26] S.A. Grant, A. Salehzadeh, Calculation of temperature effects on wetting coefficients of porous solids and their capillary pressure functions, Water Resour. Res. 32 (2) (1996) 261–270.
[27] J. Grifoll, J.M. Gastó, Y. Cohen, Non-isothermal soil water transport and evaporation, *Adv. Water Res*ources 28 (11) (2005) 1254–1266.
[28] D. Hillel, Fundamentals of soil physics, Academic Press Inc., NewYork, 2013.
[29] H. Holmberg, J. Acuña, E. Næss, O.K. Sønju, Thermal evaluation of coaxial deep borehole heat exchangers, Renewable Energy 97 (2016) 65–76.
[30] H.M. Iezzoni, J.S. McCartney, Calibration of capacitance sensors for compacted silt in non-isothermal applications, Geotech. Test. J. 39 (2) (2015) 169–180.
[31] N. Lu, Y. Dong, Closed-form equation for thermal conductivity of unsaturated soils at room temperature, J. Geotech. Geoenviron. Eng. 141 (6) (2015) 04015016.
[32] Q. Lu, G.A. Narsilio, Cost effectiveness of energy piles in residential dwellings in Australia, Current Trends Civ. Struct. Eng. 3 (3) (2019) 1–6.
[33] M.V. Lurie (Ed.), Modeling of Oil Product and Gas Pipeline Transportation, Wiley-VCH Verlag, Berlin, 2008.
[34] C. Ma, A. Di Donna, D. Dias, T. Zhang, Thermo-hydraulic and sensitivity analyses on the thermal performance of energy tunnels, Energy Build. 249 (2021) 111206, https://doi.org/10.1016/j.enbuild.2021.111206.
[35] Q. Ma, P. Wang, Underground solar energy storage via energy piles, Appl. Energy 261 (2020) 114361, https://doi.org/10.1016/j.apenergy.2019.114361.
[36] J.S. McCartney, K.D. Murphy, Investigation of potential dragdown/uplift effects on energy piles, Geomech. Energy Environ. 10 (2017) 21–28.
[37] R.J. Millington, J.M. Quirk, Permeability of porous solids, Faraday Soc. Trans. 57 (1961) 1200–1207.
[38] T. Mimouni, L. Laloui, Behaviour of a group of energy piles, Can. Geotech. J. 52 (12) (2015) 1913–1929.
[39] J.L. Monteith, M.H. Unsworth, Principles of Environmental Physics, Routledge Chapman and Hall, New York, 1990.
[40] A. Moradi, K.M. Smits, N. Lu, J.S. McCartney, Heat transfer in unsaturated soil with application to borehole thermal energy storage, Vadose Zone J. 15 (10) (2016) 1–17.
[41] C.G. Olgun, J.S. McCartney, Outcomes from the International Workshop on Thermoactive Geotechnical Systems for Near-Surface Geothermal Energy: From Research to Practice, J. Deep Found. Inst. 8 (2) (2014) 58–72.
[42] J. Nussbicker-Lux, The BTES project in Crailsheim (Germany) – monitoring results, in: Proc. 12th Int. Conf. On Energy Storage - Innostock, IEA Press, Paris, 2012, pp. 1-10.
[43] H. Park, S.-R. Lee, S. Yoon, J.-C. Choi, Evaluation of thermal response and performance of PHC energy pile: Field experiments and numerical simulation, Appl. Energy 103 (2013) 12–24.
[44] S. Park, C. Sung, K. Jung, B. Sohn, A. Chauchois, H. Choi, Constructability and heat exchange efficiency of large diameter cast-in-place energy piles with various configurations of heat exchange pipe, Appl. Therm. Eng. 90 (2015) 1061–1071.
[45] J.R. Philip, D.A. de Vries, Moisture movement in porous materials under temperature gradients, Eos, Trans. Am. Geophys. Union 38 (2) (1957) 222–232.
[46] E. Ravera, M. Sutman, L. Laloui, Cyclic thermomechanical response of fine-grained soil– concrete interface for energy piles applications, Can. Geotech. J. 58 (8) (2021) 1216–1230.
[47] A.F. Rotta Loria, L. Laloui, Thermally induced group effects among energy piles, Géotechnique 67 (5) (2017) 374–393.
[48] A.F. Rotta Loria, L. Laloui, Group action effects caused by various operating energy piles, Géotechnique 68 (9) (2018) 834–841.
[49] H. Saito, J. Šimůnek, B.P. Mohanty, Numerical analysis of coupled water, vapor, and heat transport in the vadose zone, Vadose Zone J. 5 (2) (2006) 784–800.
[50] D. Salciarini, F. Ronchi, E. Cattoni, C. Tamagnini, Thermomechanical effects induced by energy piles operation in a small piled raft, Int. J. Geomech. 15 (2) (2015) 04014042.
[51] A.K. Sani, R.M. Singh, T. Amis, I. Cavarretta, A review on the performance of geothermal energy pile foundation, its design process and applications, Renew. Sustain. Energy Rev. 106 (2019) 54–78.
[52] A.K. Sani, R.M. Singh, Response of unsaturated soils to heating of geothermal energy pile, Renewable Energy 147 (2020) 2618–2632.
[53] A.K. Sani, R.M. Singh, Long-term thermal performance of group of energy piles in unsaturated soils under cyclic thermal loading, Energies 14 (14) (2021) 4122.
[54] H.Y. She, B.E. Sleep, The effect of temperature on capillary pressure-saturation relationships for air-water and perchloroethylene-water systems, Water Resour. Res. 34 (10) (1998) 2587–2597.
[55] B. Sibbitt, D. McClenahan, R. Djebbar, J. Thornton, B. Wong, J. Carriere, J. Kokko, The performance of a high solar fraction seasonal storage district heating system–five years of operation, Energy Proc. 30 (2012) 856–865.
[56] K.M. Smits, A. Cihan, T. Sakaki, T.H. Illangasekare, Evaporation from soils under thermal boundary conditions: Experimental and modeling investigation to compare equilibrium-and nonequilibrium-based approaches, Water Resour. Res. 47 (5) (2011) 1–14.
[58] M.A. Stewart, J.S. McCartney, Centrifuge modeling of soil-structure interaction in energy foundations, J. Geotech. Geoenviron. Eng. 140 (4) (2014) 04013044.
[59] H.R. Thomas, S.D. King, Coupled temperature/capillary potential variations in unsaturated soil, J. Eng. Mech. 117 (11) (1991) 2475–2491.
[60] H.R. Thomas, Y. He, Analysis of coupled heat, moisture and air transfer in a deformable unsaturated soil, Géotechnique 45 (4) (1995) 677–689.
[61] H.R. Thomas, Y. He, A coupled heat–moisture transfer theory for deformable unsaturated soil and its algorithmic implementation, Int. J. Numer. Meth. Eng. 40 (18) (1997) 3421–3441.
[62] H.R. Thomas, H. Missoum, Three-dimensional coupled heat, moisture, and air transfer in a deformable unsaturated soil, Int. J. Numer. Meth. Eng. 44 (7) (1999) 919–943.
[63] G.C. Topp, J.L. Davis, A.P. Annan, Electromagnetic determination of soil water content: Measurements in coaxial transmission lines, Water Resources 16 (3) (1980) 574–582.
[64] M.T. van Genuchten, A closed-form equation for predicting the hydraulic conductivity of unsaturated soils, SSSA 44 (5) (1980) 892–898.
[65] B. Wang, A. Bouazza, R.M. Singh, C. Haberfield, D. Barry-Macaulay, S. Baycan, Posttemperature effects on shaft capacity of a full-scale geothermal energy pile, J. Geotech. Geoenviron. Eng. 141 (4) (2015) 04014125.
[66] Z. Wang, F. Wang, J. Liu, Z. Ma, E. Han, M. Song, Field test and numerical investigation on the heat transfer characteristics and optimal design of the heat exchangers of a deep borehole ground source heat pump system, Energy Convers. Manage. 153 (2017) 603–615.
[67] A. Wayllace, N. Lu, A transient water release and imbibitions method for rapidly measuring wetting and drying soil water retention and hydraulic conductivity functions, Geotech. Test. J. 35 (1) (2012) 103–117.
[68] B. Welsch, W. Rühaak, D.O. Schulte, K. Bear, S. Homuth, I. Sass, Comparative study of medium deep borehole thermal energy storage systems using numerical modelling, Proc. World Geothermal Congress 2015, International Geothermal Association, Bochum, 2015, pp. 1-6.
[69] S. Whitaker, Simultaneous heat, mass, and momentum transfer in porous media: a theory of drying, Adv. Heat Transfer. 13 (1977) 119–203.
[70] S. You, X. Cheng, H. Guo, Z. Yao, Experimental study on structural response of CFG energy piles, Appl. Therm. Eng. 96 (2016) 640–651.
[71] J. Zhang, A.K. Datta, Some considerations in modeling of moisture transport in heating of hygroscopic materials, Drying Technol. 22 (8) (2004) 1983–2008.
[72] J. Zhao, H. Wang, X. Li, C. Dai, Experimental investigation and theoretical model of heat transfer of saturated soil around coaxial ground coupled heat exchanger, Appl. Therm. Eng. 28 (2-3) (2008) 116–125.
[73] K.D. Murphy, J.S. McCartney, K.S. Henry, Evaluation of thermo-mechanical and thermal behavior of full-scale energy foundations, Acta Geotech. 10 (2) (2015) 179–195.
[74] L. Laloui, M. Nuth, L. Vulliet, Experimental and numerical investigations of the behaviour of a heat exchanger pile, Int. J. Numer. Anal. Methods. Geomechan. 30 (2006) 763–781.
[75] W. Wang, R. Regueiro, J.S. McCartney, Coupled axisymmetric thermo-poro-elasto-plastic finite element analysis of energy foundation centrifuge experiments in partially saturated silt, Geotech. Geol. Eng. 33 (2) (2015) 373–388.